Evaluating specific error characteristics of microwave-derived cloud liquid water products

Thomas J. Greenwald,[1] Tristan S. L'Ecuyer,[2] and Sundar A. Christopher[3]

Received 3 July 2007; revised 14 September 2007; accepted 22 October 2007; published 21 November 2007.

[1] Methods are presented for assessing minimum errors and cloud inhomogeneity effects in cloud liquid water path (LWP) products derived from passive microwave satellite measurements. Using coincident visible/infrared satellite data, errors are isolated by identifying certain cloud conditions within the microwave sensor's field of view. Analysis of 3 weeks of global pixel-level LWP data revealed that 70% of the systematic errors occurred between -0.011 and $+0.025$ kgm^{-2}, with the mean random error being 0.013 kgm^{-2}. For overcast clouds these systematic errors translate to a mean lower-bound relative error of about +23%. A significant correlation of these products with near-surface wind speed was also shown. The LWP products were found to depend on cloud fraction as well, suggesting the influence of beam filling errors. This approach shows promise in characterizing the minimum errors in LWP products needed for climate and remote sensing studies as well as future data assimilation applications. **Citation:** Greenwald, T. J., T. S. L'Ecuyer, and S. A. Christopher (2007), Evaluating specific error characteristics of microwave-derived cloud liquid water products, *Geophys. Res. Lett.*, *34*, L22807, doi:10.1029/2007GL031180.

1. Introduction

[2] Measurements from passive microwave sensors on satellites have provided over two decades of continuous cloud liquid water path (LWP) (liquid water content integrated vertically through the atmospheric column) products over the oceans. These datasets are the longest running and most complete observations of cloud microphysical properties available and are unique also in that they are free of the effects of most ice particles, are derived independently of droplet size information (unlike optical methods), and are available day or night.

[3] Despite the use of these products in a broad range of studies, from climate model validation to cloud-radiation interaction [e.g., *Stephens and Greenwald*, 1991; *Zuidema and Hartmann*, 1995; *Chen and Roeckner*, 1997; *Borg and Bennartz*, 2007; *Ming et al.*, 2007], little is known regarding their error characteristics. Direct comparisons against in situ and surface-based microwave observations have yielded promising results for limited cases [*Greenwald et al.*, 1993; *Cober et al.*, 1996; *Prigent et al.*, 1997; *Offiler et al.*, 1998]; however, aircraft measurements have sample size and representativeness issues, as well as being relatively rare and costly; whereas observations from surface-based microwave radiometers can exhibit significant systematic errors [*Turner et al.*, 2007].

[4] Knowledge of LWP errors is especially relevant to studies of cloud properties and radiation. For example, cloud LWP uncertainties constitute one of the largest error sources in simulating the Earth's radiation budget [*L'Ecuyer and Stephens*, 2003]. The sensitivity of top-of-atmosphere (TOA) and surface radiative fluxes to LWP is highest for thin water clouds (LWP < 0.05 kgm^{-2}), thus placing an unusually high demand on LWP accuracy [*Sengupta et al.*, 2003; *Turner et al.*, 2007]. In satellite remote sensing of cloud droplet number concentration, LWP uncertainties are one of the dominant retrieval errors [*Bennartz*, 2007]. Not only are LWP error estimates needed for climate studies and remote sensing, but also for defining satellite instrument requirements for measuring global climate change [*Ohring et al.*, 2005].

[5] This study proposes an independent way of interpreting and quantifying certain error characteristics of cloud LWP products globally using concurrent data from visible/infrared satellite sensors. The approach draws mainly from studies that examined LWP data in cloud-cleared scenes [e.g., *Liu and Curry*, 1993; *Lin and Rossow*, 1994; *Jung et al.*, 1998] but it also examines both overcast and inhomogeneous cloud situations. Other potentially significant error sources not considered in this study include cloud emission temperature uncertainties [*Greenwald et al.*, 1993] and possible undetected rain contamination [*Wentz and Spencer*, 1998].

[6] This work improves upon and extends earlier studies by 1) utilizing better collocation, 2) investigating sub-field-of-view (FOV) cloud effects, 3) distinguishing between systematic and random errors, and 4) showing how cloud-cleared errors impact the cloudy-sky LWP products. Detailed collocation techniques are essential since extracting maximum error information requires accurate determination of cloud conditions within the microwave sensor's FOV.

2. Satellite Data

[7] The sources of satellite data are the Advanced Microwave Scanning Radiometer-E (AMSR-E) and the MODerate resolution Imaging Spectroradiometer (MODIS) on the Aqua platform. As part of NASA's A-train, Aqua resides in a low earth orbit with equatorial crossing times of about 1:30 AM and 1:30 PM local time. This study uses Level 2 (i.e., swath or pixel-level) data products for the period 1–21 July 2002. The duration of the study period was largely dictated by the enormous data volume and computational

[1] Cooperative Institute for Meteorological Satellite Studies, University of Wisconsin–Madison, Madison, Wisconsin, USA.
[2] Department of Atmospheric Science, Colorado State University, Fort Collins, Colorado, USA.
[3] Department of Atmospheric Science, University of Alabama in Huntsville, Huntsville, Alabama, USA.

0094-8276/07/2007GL031180$05.00

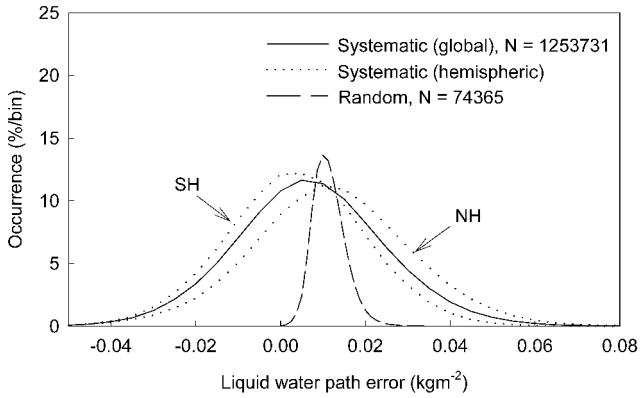

Figure 1. Error distributions for instantaneous cloud-cleared AMSR cloud liquid water path products for July 1–21 2002. N is number of data points, NH is Northern Hemisphere and SH is Southern Hemisphere. Bin size is 0.005 kgm^{-2}.

resources required to perform pixel-level matches of the two datasets.

[8] AMSR-E is a conical-scanning passive microwave instrument with twelve dual-polarization channels at 6.9, 10.7, 18.7, 23.8, 36.5, and 89 GHz. The Version 1 AMSR-E ocean products include near-surface wind speed, LWP, sea surface temperature (SST), rainfall rate, and total precipitable water (TPW). These products are retrieved from all channels except 89 GHz [*Wentz and Meissner*, 2000]. The LWP products have an effective spatial resolution of 14 × 8 km. To greatly reduce the effect of precipitation on the analyses, the LWP data were filtered using the rainfall product quality flags. While use of these flags will not eliminate all rain events, they will remove events having the greatest impact.

[9] MODIS is a cross-track-scanning imager with 36 channels ranging from 0.4 to 14.5 μm. The Collection 4 cloud products, which are at 1 km resolution, were used. Products relevant to this study include cloud mask data, visible optical depth, effective particle radius, identification of cloud phase, and infrared (channel 31, 11 μm) window brightness temperatures. *Platnick et al.* [2003] discusses the retrieval algorithms used in generating these cloud products.

[10] Also used for comparison is cloud LWP inferred from visible optical depth (τ) and effective radius (r_e) products. For an adiabatically stratified cloud [e.g., *Borg and Bennartz*, 2007] the cloud LWP is obtained as

$$LWP = \frac{5}{9} r_e \tau \rho_w$$

where ρ_w is the density of liquid water.

3. Approach

[11] The method of collocation is the most important aspect of combining pixel-level microwave-derived LWP products and visible/infrared imager data. Since cloud detection is more reliable with multi-spectral data, collocations are limited to local daytime scenes. Our approach is to first search for the MODIS pixel nearest to the center of a given AMSR-E FOV. All MODIS pixels that fall within the AMSR-E's elliptically shaped footprint are then identified taking care to precisely account for the different viewing geometries of each instrument.

[12] For each collocation a number of MODIS products are saved. Quantities related to temperature include the 11-μm brightness temperature (average, cloud only average, and minimum) and average cloud top temperature. Cloud properties include average visible optical depth, effective radius, and water path. All quantities are averaged over the AMSR-E FOV assuming a 2-D Gaussian shaped antenna function with the maximum at the center of the FOV. Other important quantities saved include the cloud fraction and number of liquid, ice, and mixed phase clouds within each FOV.

[13] Key to isolating errors in the cloud LWP products is restricting the analyses to certain cloud conditions. The first are cloud-cleared scenes, where the variability and biases in the LWP products are a direct measure of the uncertainty in non-cloud related properties, such as atmospheric absorption (both oxygen and water vapor), and sea surface emissivity and temperature. These uncertainties establish lower bounds on the LWP product errors. The retrieved cloud LWP for a given cloud-cleared FOV defines the systematic error since the true LWP should be exactly or very nearly zero. Random errors, on the other hand, are computed as the spatial standard deviation of cloud-cleared LWP products for small regions (0.5° × 0.5°) at a given time.

[14] For cloudy scenes, the special case of overcast conditions within the FOV is considered. Overcast situations are relatively homogeneous and for liquid only clouds allow for direct comparisons with optically derived cloud LWP [e.g., *Lin and Rossow*, 1994; *Greenwald et al.*, 1997; *Horváth and Davies*, 2007; *Borg and Bennartz*, 2007.] Owing to visible optical depths being typically two orders of magnitude greater than microwave optical depths, optical methods are far more sensitive to changes in very small LWP. However these methods are subject to the plane-parallel bias (i.e., due to unresolved small-scale variability [*Cahalan et al.*, 1994]) and are more prone to 3D effects, though in locally overcast conditions 3D effects are somewhat reduced. Uncertainties due to vertical cloud inhomogeneities and aerosol contamination are generally second order influences on optical methods.

[15] Finally, examining cloud LWP products in broken cloud scenes can yield insight into the effect of inhomogeneous clouds on microwave sensors [*Miletta and Katsaros*, 1995; *Greenwald et al.*, 1997]. Because the spatial resolution of these sensors is too coarse to resolve individual cloud elements, the mixture of cloudy and clear sky conditions within the FOV can lead to what is often called "beam-filling error", a bias that reduces the observed brightness temperature and, hence, underestimates the retrieved cloud LWP [*Bremen et al.*, 2002].

4. Results

4.1. Cloud Cleared and Overcast

[16] Figure 1 shows that systematic errors for cloud-cleared LWP data are normally distributed but slightly offset from zero. This offset may suggest a small calibration error in the AMSR 37 GHz brightness temperature data. The

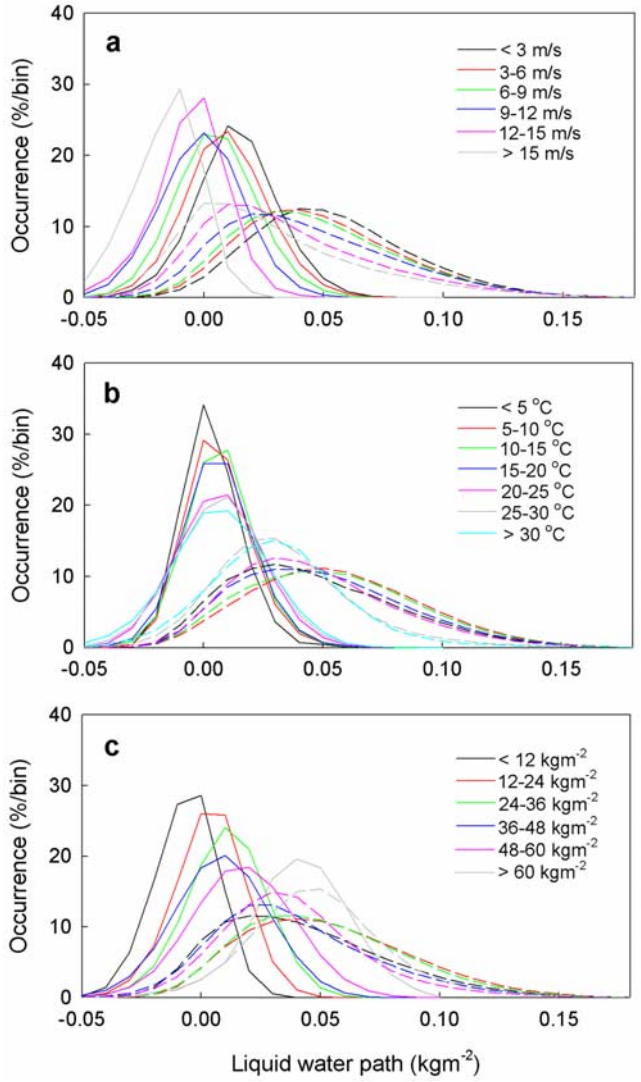

Figure 2. Distributions of instantaneous cloud-cleared (solid) and nonprecipitating overcast (dashed) AMSR-E cloud liquid water path products stratified into different (a) wind speed, (b) sea surface temperature and (c) total precipitable water categories. Bin size for both cloud-cleared and overcast data is 0.01 kgm^{-2}.

mean error is +0.0070 kgm^{-2} and 70% of the errors lie between −0.011 and +0.025 kgm^{-2}. The errors also exhibit hemispheric differences of +0.012 kgm^{-2} for the north and +0.0036 kgm^{-2} for the south.

[17] Random errors, on the other hand, behave much like a gamma distribution and have a mean error of 0.013 kgm^{-2} and a mode of 0.010 kgm^{-2}. The time-mean geographic distribution of random errors (not shown) resembles the mean distribution of cloud-cleared TPW (i.e., errors generally increase with TPW); a result not unexpected since water vapor has a major impact on the cloud LWP products.

[18] To better understand the nature of these systematic errors, the cloud-cleared LWP distributions were binned according to different broad ranges of AMSR-derived wind speed, SST, and TPW. This technique has been used by *Wentz and Meissner* [2000] to identify false correlations among different microwave-derived products. Ideally, one would prefer errors to be independent of these other quantities.

[19] Figure 2 reveals that the cloud-cleared LWP data are relatively independent of SST, but there is a strong systematic dependence on wind speed and a somewhat less distinct trend with TPW. Since the northern hemisphere during summer typically has larger TPW and lower wind speeds than the southern and because errors are negatively correlated with wind speed and generally positively correlated with TPW, this may explain the hemispheric differences seen in Figure 1.

[20] But are these same dependencies reflected in the LWP products under cloudy conditions? Applying the same analysis to LWP data for overcast clouds, but limited to a minimum 11-μm T_b of >255 K within the FOV, shows the same dependence on wind speed (see Figure 2). This correspondence is linearly correlated at 0.98 when considering the mean values of the cloud-cleared and overcast distributions. The dependence of overcast LWP data on TPW is less clear but there is a separation in the distributions between the lowest and highest TPW categories in terms of both the mean and the mode values.

[21] The relative impact of these errors on overcast LWP data cannot be evaluated on an instantaneous basis. However, this impact can be estimated in a time-space mean sense by averaging the cloud-cleared and overcast LWP data used in Figure 2 separately over the 3-week period on $1^\circ \times 1^\circ$ grids. For example, the relative systematic error in overcast LWP at a grid point is obtained by dividing the average cloud-cleared LWP by the average overcast LWP. The mean relative systematic error for overcast LWP was found to be +23% with 70% of the values lying between −8.2% and +54%. Applying a similar analysis using the cloud-cleared random errors yielded a mean relative random error in the overcast LWP of 42%. The significantly larger relative random error is due to the tendency of these errors to be largest in widespread areas where the overcast LWP is smallest.

[22] Comparison of AMSR-E and MODIS LWP data for AMSR-E FOVs with warm (i.e., 11-μm T_b > 273 K) overcast clouds is also revealing (Figure 3). While the mean values are nearly identical (0.0511 versus 0.0515 kgm^{-2})

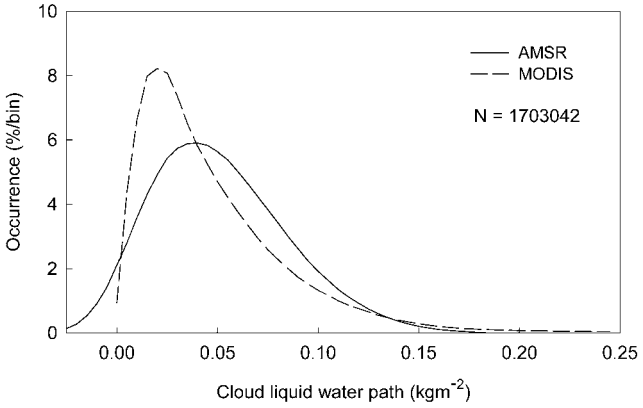

Figure 3. Distributions of nonprecipitating warm overcast liquid water path derived from instantaneous AMSR-E and MODIS data. N is number of data points. Bin size is 0.005 kgm^{-2}.

the shapes of the distributions are quite different. The distinctly broader AMSR-E LWP distribution is likely caused by both the wind speed/TPW dependencies described earlier and the reduced sensitivity of 37 GHz measurements to small LWP. However, possible biases in the MODIS LWP data cannot be ruled out as a cause of some of these differences.

4.2. Non-Overcast Cloudy Scenes

[23] To investigate the effect of scattered clouds on the AMSR-E LWP products, the analysis was limited to warm clouds. This was done to more directly relate cloud amount within the FOV to mean cloud LWP since the presence of ice or mixed-phase clouds will bias the cloud amount.

[24] Results in Figure 4 indicate a trend of decreasing cloud LWP with decreasing cloud amount (see also Table 1), similar to the findings of *Greenwald et al.* [1997]. This systematic reduction in cloud LWP may be due mainly to the beam-filling effect, though it is uncertain how other factors might influence this relationship, such as the possibility that the LWP of individual cloud elements may decrease as the cloud field becomes more broken.

[25] Not only does a strong correlation exist between cloud LWP and cloud amount, the results also suggest a difference between the LWP of scattered clouds with those of locally (~10 km scale) overcast clouds. Even assuming that LWP differences for nonovercast clouds are due entirely to beam-filling errors and then scaling the LWP by cloud amount but only for values above 25% [see *Greenwald et al.*, 1997], indicates the adjusted cloud LWP data are still significantly smaller (14–39%) than the overcast cloud LWP.

5. Conclusions

[26] Methods for estimating minimum errors in microwave-based cloud LWP products have been presented. Applying these techniques to 3 weeks of global AMSR-E pixel-level LWP data has shown that 70% of their systematic errors occurred between -0.011 and $+0.025$ kgm^{-2} (-8.2% and $+54\%$) with an average random error of 0.013 kgm^{-2}. Investigation of LWP data in inhomogeneous cloud conditions also showed a dependence of the data on cloud fraction, suggesting the influence of beam filling errors. Most troubling, however, was a strong dependence of the products on surface wind speed, which contributed significantly in reducing their sensitivity for small LWP. This deficiency, along with an implicit dependence of LWP on cloud amount, presents challenges in interpreting these datasets for climate studies.

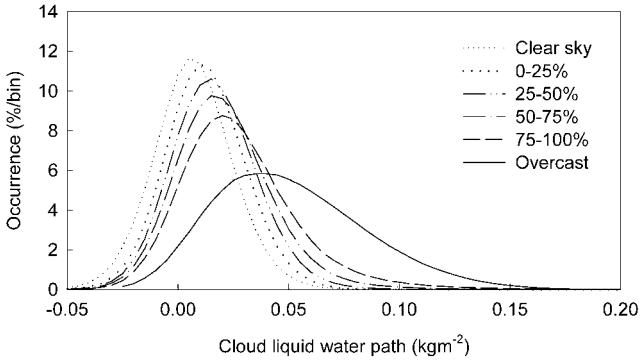

Figure 4. Distributions of nonprecipitating warm overcast cloud liquid water path from instantaneous AMSR-E data stratified into different cloud amount categories. Bin size is 0.005 kgm^{-2}.

Table 1. Cloud Statistics for AMSR-E Liquid Water Path (LWP) Data Analysis in Non-Overcast Cloud Conditions

Cloud Amount Range	Number of Data Points	Mean Cloud LWP, kgm^{-2}	Mean Cloud Amount
0–25%	880491	0.0125	11.4%
25–50%	698514	0.0166	37.5%
50–75%	720735	0.0212	62.7%
75–100%	945751	0.0276	88.5%

[27] The errors reported in this study, while seemingly small, will have an important impact on radiation budget calculations. Assuming a mean cloud LWP of 0.05 kgm^{-2} (based on Figure 3), a +0.025 kgm^{-2} perturbation in LWP yields a +75 Wm^{-2} change in TOA shortwave (SW) flux and a -87 Wm^{-2} change in surface SW flux [*Turner et al.*, 2007]. In terms of cloud radiative forcing (CRF), a +0.025 kgm^{-2} perturbation translates roughly to a -13 Wm^{-2} change in the net CRF [*Greenwald et al.*, 1995].

[28] Even if uncertainties due to the surface wind speed dependence could be significantly reduced, there is a far greater potential in producing higher quality LWP products by exploiting measurements near 85 GHz. Because these measurements are more sensitive to smaller liquid water amounts, it has been shown that including these data can greatly reduce both systematic and random errors in LWP retrievals [*Jung et al.*, 1998].

[29] Finally, the drawback of using multi-sensor satellite data is the time consuming analysis due to the massive datasets involved. However, new processing systems composed of computer clusters and dedicated software will enable the processing of one month of satellite data in just one day [*Gumley et al.*, 2006]. These systems will make multi-sensor satellite collocation feasible and provide long-term global estimates of minimum errors in cloud LWP products not only for climate and remote sensing studies, but also for future assimilation of these observations into forecast models.

[30] **Acknowledgments.** Special thanks go to Graeme Stephens at Colorado State University for planting the seed for this study. MODIS cloud products were obtained from the Goddard Space Flight Center DAAC. Remote Sensing Systems provided the AMSR-E Ocean Products. Comments from two anonymous reviewers are also appreciated.

References

Bennartz, R. (2007), Global assessment of marine boundary layer cloud droplet number concentration from satellite, *J. Geophys. Res.*, *112*, D02201, doi:10.1029/2006JD007547.

Borg, L. A., and R. Bennartz (2007), Vertical structure of stratiform marine boundary layer clouds and its impact on cloud albedo, *Geophys. Res. Lett.*, *34*, L05807, doi:10.1029/2006GL028713.

Bremen, L. V., E. Ruprecht, and A. Macke (2002), Errors in liquid water path retrieval arising from cloud inhomogeneities: The beam-filling effect, *Meteorol. Z.*, *11*, 13–19.

Cahalan, R. F., W. Ridgway, W. J. Wiscombe, and T. L. Bell (1994), The albedo of fractal stratocumulus clouds, *J. Atmos. Sci.*, *51*, 2434–2455.

Chen, C. T., and E. Roeckner (1997), Cloud simulations with the Max Planck Institute for Meteorology general circulation model ECHAM4 and comparisons with observations, *J. Geophys. Res.*, *102*, 9335–9350.

Cober, S. G., A. Tremblay, and G. A. Isaac (1996), Comparisons of SSM/I liquid water paths with aircraft measurements, *J. Appl. Meteorol.*, *35*, 503–520.

Greenwald, T. J., G. L. Stephens, T. H. Vonder Haar, and D. L. Jackson (1993), A physical retrieval of cloud liquid water over the global oceans using Special Sensor Microwave/Imager (SSM/I) observations, *J. Geophys. Res.*, *98*, 18,471–18,488.

Greenwald, T. J., G. L. Stephens, S. A. Christopher, and T. H. Vonder Haar (1995), Observations of the global characteristics and regional radiative effects of marine cloud liquid water, *J. Clim.*, *8*, 2928–2946.

Greenwald, T. J., S. A. Christopher, and J. Chou (1997), Cloud liquid water path comparisons from passive microwave and solar reflectance satellite measurements: Assessment of sub-field-of-view cloud effects in microwave retrievals, *J. Geophys. Res.*, *102*, 19,585–19,596.

Gumley, L. E., H. Revercomb, P. Antonelli, B. Baum, and R. Holz (2006), The NPP Atmosphere Product Evaluation and Test Element (PEATE), paper presented at 12th Conference on Atmospheric Radiation, Am. Meteorol. Soc., Madison, Wisc., 9–14 July.

Horváth, Á., and R. Davies (2007), Comparison of microwave and optical cloud water path estimates from TMI, MODIS, and MISR, *J. Geophys. Res.*, *112*, D01202, doi:10.1029/2006JD007101.

Jung, T., E. Ruprecht, and F. Wagner (1998), Determination of cloud liquid water path over the oceans from Special Sensor Microwave/Imager (SSM/I) data using neural networks, *J. Appl. Meteorol.*, *37*, 832–844.

L'Ecuyer, T. S., and G. L. Stephens (2003), The tropical oceanic energy budget from the TRMM perspective. Part I: Algorithm and uncertainties, *J. Clim.*, *16*, 1967–1985.

Lin, B., and W. B. Rossow (1994), Observations of cloud liquid water over oceans: Optical and microwave remote sensing methods, *J. Geophys. Res.*, *99*, 20,907–20,927.

Liu, G., and J. A. Curry (1993), Determination of characteristic features of cloud liquid water from satellite microwave measurements, *J. Geophys. Res.*, *98*, 5069–5092.

Miletta, J., and K. B. Katsaros (1995), Using coincident multispectral satellite data to assess the accuracy of special sensor microwave imager liquid water path measurements, *J. Geophys. Res.*, *100*, 16,333–16,339.

Ming, Y., V. Ramaswamy, L. J. Donner, V. T.J. Phillips, S. A. Klein, P. A. Ginoux, and L. W. Horowitz (2007), Modeling the interactions between aerosols and liquid water clouds with a self-consistent cloud scheme in a general circulation model, *J. Atmos. Sci.*, *64*, 1189–1209.

Offiler, D., L. Eymard, D. Kilham, E. Gérard, and H. Gaeng (1998), Cloud Retrieval Validation Experiment (CLOREVAL) final report, rapport pour la commission Européenne, programme Environnement et Climat, Met Off., Exeter, U. K., Sept.

Ohring, G., B. Wielicki, R. Spencer, B. Emery, and R. Datla (2005), Satellite instrument calibration for measuring global climate change, *Bull. Am. Meteorol. Soc.*, *86*, 1303–1313.

Platnick, S., M. D. King, S. A. Ackerman, W. P. Menzel, B. A. Baum, C. Riedl, and R. A. Frey (2003), The MODIS cloud products: Algorithms and examples from Terra, *IEEE Trans. Geosci. Remote Sens.*, *41*, 459–473.

Prigent, C., L. Phalippou, and S. English (1997), Variational inversion of the SSM/I observations during the ASTEX campaign, *J. Appl. Meteorol.*, *36*, 493–508.

Sengupta, M., E. E. Clothiaux, T. P. Ackerman, S. Kato, and Q. Min (2003), Importance of accurate liquid water path for estimation of solar radiation in warm boundary layer clouds: An observational study, *J. Clim.*, *16*, 2997–3009.

Stephens, G. L., and T. J. Greenwald (1991), The Earth's radiation budget in relation to atmospheric hydrology: 2. Observations of cloud effects, *J. Geophys. Res.*, *96*, 15,325–15,340.

Turner, D. D., et al. (2007), Thin liquid water clouds: Their importance and our challenge, *Bull. Am. Meteorol. Soc.*, *88*, 177–190.

Wentz, F. J., and T. Meissner (2000), AMSR Ocean Algorithm Theoretical Basis Document (ATBD), *RSS Tech. Doc.* 121599*A*-1, Remote Sens. Syst., Santa Rosa, Calif. (Available at http://eospso.gsfc.nasa.gov)

Wentz, F. J., and R. W. Spencer (1998), SSM/I rain retrievals within a unified all-weather algorithm, *J. Atmos. Sci.*, *55*, 1613–1627.

Zuidema, P., and D. L. Hartmann (1995), Satellite determination of stratus cloud microphysical properties, *J. Clim.*, *8*, 1638–1657.

S. A. Christopher, Department of Atmospheric Science, University of Alabama in Huntsville, Huntsville, AL 35805, USA.

T. S. L'Ecuyer, Department of Atmospheric Science, Colorado State University, Fort Collins, CO 80523, USA.

T. J. Greenwald, Cooperative Institute for Meteorological Satellite Studies, University of Wisconsin–Madison, Madison, WI 53706, USA. (tomg@ssec.wisc.edu)